Title
Observations of Cl_2, Br_2, and I_2 in coastal marine air

Journal
Journal of Geophysical Research, 113(D21)

ISSN
0148-0227

Authors
Finley, B. D
Saltzman, E. S

Publication Date
2008-11-01

DOI
10.1029/2008JD010269

Observations of Cl_2, Br_2, and I_2 in coastal marine air

B. D. Finley[1] and E. S. Saltzman[1]

Received 14 April 2008; revised 11 July 2008; accepted 4 August 2008; published 4 November 2008.

[1] Cl_2, Br_2, and I_2 were measured in coastal Pacific air from 2 to 29 January 2006. Air was sampled at 10 m over the sea surface near the end of Scripps Pier (La Jolla, California). The measurements were made using atmospheric pressure chemical ionization with tandem mass spectrometry (APCI/MS/MS). Over the course of this study, Cl_2, Br_2, and I_2 levels ranged from below detection limits of 1.0, 0.5, and 0.2 ppt, respectively, to maxima of 26, 19, and 8 ppt, respectively. Mean dihalogen levels for the study period were 2.3 ± 1 ppt for Cl_2, 2.3 ± 0.4 ppt for Br_2, and 0.7 ± 0.1 ppt for I_2 (expressed as geometric mean ±1 geometric standard error). The mixed dihalogens BrCl, ICl, and IBr had geometric mean levels below 0.3 ± 1 ppt and never exceeded their detection limits of 0.5 ppt. Consistent patterns of diurnal variability were observed for Cl_2 and I_2, with Cl_2 maxima during daytime and I_2 appearing almost exclusively at night. The detection of I_2 appeared to be related to the passage of air over nearby kelp beds. The observed dihalogen levels suggest that (1) chlorine atom oxidation of hydrocarbons makes a significant contribution to the formation of ozone and (2) halogen atom oxidation of airborne mercury contributes to mercury deposition in polluted coastal air.

Citation: Finley, B. D., and E. S. Saltzman (2008), Observations of Cl_2, Br_2, and I_2 in coastal marine air, *J. Geophys. Res.*, *113*, D21301, doi:10.1029/2008JD010269.

1. Introduction

[2] In the atmosphere, chlorine, bromine, and iodine atoms can participate in catalytic ozone destruction cycles involving the formation and recycling of weakly bonded halogen oxides. In polluted regions, oxidation of hydrocarbons by chlorine atoms can also lead to ozone formation through the production of peroxy radicals and resulting conversion of NO to NO_2. The abundance of halogen radicals in the troposphere is not well documented and their role in tropospheric photochemistry is not well understood. The coastal boundary layer is an environment where halogen photochemistry is potentially important because of the abundance of marine aerosols and the interaction of marine air with polluted air over populated regions.

[3] Indirect evidence from several sources suggests chlorine atom concentrations can reach levels within an order of magnitude of OH levels [*Keene et al.*, 1993; *Singh et al.*, 1996; *Volpe et al.*, 1998; *Dickerson et al.*, 1999; *Ayers et al.*, 1999; *Wingenter et al.*, 1999; *Johansen et al.*, 2000; *Pszenny et al.*, 2004]. Direct evidence of reactive chlorine in the boundary layer comes from the spectroscopic detection of ClO [*Stutz et al.*, 2002], measurements of unique products from the Cl + isoprene reaction [*Tanaka et al.*, 2003], and mass spectrometric measurements of Cl_2 [*Spicer et al.*, 1998]. Chlorine atom precursors in the MBL come from sea salt aerosols via acid displacement [*Eriksson*, 1959a, 1959b; *Johansen et al.*, 2000] and the release of photolytically active compounds (Cl_2, HOCl) from the bulk aerosol [*Pszenny et al.*, 1993; *Sander and Crutzen*, 1996; *Vogt et al.*, 1996]. Laboratory results show that chlorine precursors can be released from heterogeneous reactions on sea salt aerosol surfaces [*Behnke et al.*, 1997; *Oum et al.*, 1998; *Schweitzer et al.*, 1998; *Finlayson-Pitts and Hemminger*, 2000; *Knipping et al.*, 2000]. Modeling studies show chlorine to be an ozone source in polluted coastal regions [*Knipping and Dabdub*, 2002a, 2002b, 2003; *Chang et al.*, 2002].

[4] Reactive bromine has been detected as BrO in coastal marine air [*Saiz-Lopez et al.*, 2004], the eastern North Atlantic [*Leser et al.*, 2003], and downwind of salt lakes [*Stutz et al.*, 2002; *Honninger et al.*, 2004]. *Spicer et al.* [2002] detected a small signal due to Br_2 while measuring dihalogens on Long Island [*Spicer et al.*, 1998], but did not report mixing ratios. Bromine shares a sea salt aerosol source with chlorine. Coarse mode sea salt aerosols exhibit bromide depletions relative to seawater [*Ayers et al.*, 1999], although in heavily polluted air these aerosols may become enriched in bromide [*Sander et al.*, 2003]. *Fan and Jacob* [1992] and *Vogt et al.* [1996] proposed mechanisms resulting in autocatalytic release of bromine from sea salt aerosols. Modeling studies of halogen activation and sea salt chemistry suggest that the cycling of reactive brominated compounds (Br_2, HOBr) dominates over chlorinated species [*Sander and Crutzen*, 1996; *Keene et al.*, 1998; *von Glasow et al.*, 2002].

[5] Iodine radicals in the marine boundary layer are produced from photolysis of both alkyl iodides and I_2.

[1]Department of Earth System Science University of California, Irvine, California, USA.

0148-0227/08/2008JD010269

The photolysis frequencies for I_2 are significantly greater than those for iodinated hydrocarbons. Alkyl iodides are produced by macroalgae and phytoplankton in the upper ocean [*Nightingale et al.*, 1995; *Pedersèn et al.*, 1996; *Carpenter et al.*, 1999, 2001] and have been detected in the MBL [*Schall and Heumann*, 1993; *Carpenter et al.*, 1999]. Laboratory studies have shown kelp to be a source of I_2 [*Truesdale and Canosamas*, 1995; *Kupper et al.*, 1998; *Palmer et al.*, 2005]. I_2 has been detected spectroscopically in air near coastal kelp beds [*Saiz-Lopez and Plane*, 2004; *Saiz-Lopez et al.*, 2006]. Reactive iodine in the form of IO and OIO has also been detected in coastal regions [*Alicke et al.*, 1999; *Allan et al.*, 2000; *Saiz-Lopez and Plane*, 2004]. Modeling studies show that both iodine and bromine can cause ozone depletion [*Sander and Crutzen*, 1996; *Davis et al.*, 1996; *Vogt et al.*, 1999; *von Glasow et al.*, 2002]. Iodine oxides have also been implicated in the rapid formation of ultrafine coastal aerosols [*O'Dowd et al.*, 2002].

[6] The oxidation of atmospheric mercury (Hg^0) to reactive gaseous mercury (RGM, Hg^{II}) has important implications for mercury cycling. Unlike elemental mercury, RGM is soluble in water and rapidly deposits to surfaces. Hg^0 is enhanced in polluted urban air relative to the global background [*Shon et al.*, 2008], and model studies of Hg have suggested that halogen oxidation of Hg^0 could be a significant source of RGM in the free troposphere [*Holmes et al.*, 2006], the marine boundary layer [*Laurier et al.*, 2003; *Hedgecock et al.*, 2003], and in polluted urban air [*Shon et al.*, 2005].

[7] This paper presents measurements of the dihalogens Cl_2, Br_2, and I_2 over the sea surface off La Jolla, California. To the best of our knowledge, these data include the first reported mixing ratios of Br_2 in the MBL outside of the Arctic and the first observations of ambient I_2 by atmospheric pressure chemical ionization tandem mass spectrometry.

2. Experiment Location, Meteorology, and Ancillary Measurements

2.1. Location

[8] Field measurements were made at the Scripps Institute of Oceanography pier facility in La Jolla, California from 2 to 29 January 2006. The pier is located at 32.87°N, −117.26°W. The pier is 330 m long and 10 m above the sea surface. The coastline at this site is oriented northeast/southwest. The instruments were housed in a small building 20 m from the end of the pier.

2.2. Meteorology

[9] Meteorological parameters, including wind speed and direction, air temperature and pressure, cloud cover, and tidal height were measured continuously at the pier. The raw data are available at http://meteora.ucsd.edu/weather. Air mass trajectories during this period were calculated using the HYSPLIT v4.7 model [*Draxler and Hess*, 1997, 1998] and meteorological data from the Eta data assimilation system (EDAS; ftp://www.arl.noaa.gov/pub/archives/).

[10] Local measurements at Scripps Pier are shown as a time series in Figure 1. Skies were clear and sunny with the exception of cloudy days on 2 and 3 January. Daytime temperatures on most days were 14–16°C (Figure 1, top).

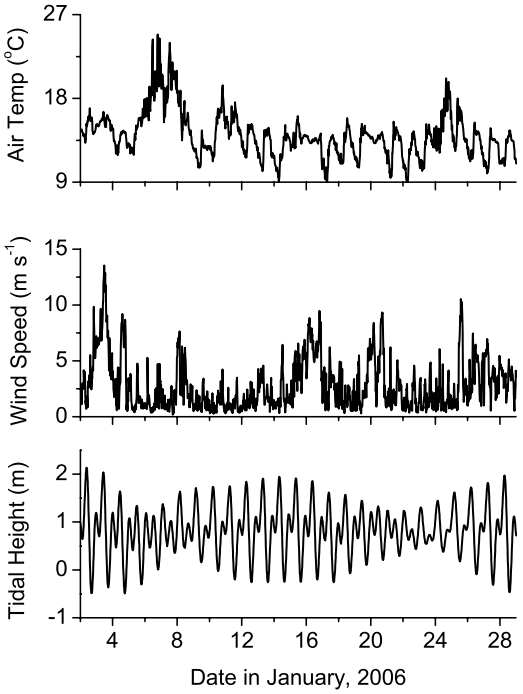

Figure 1. (top) Air temperature, (middle) wind speed, and (bottom) tidal height measured at Scripps Pier from 2 to 29 January 2006.

During 5–8 January, however, temperatures reached 22°C and did not cool off significantly at night. Temperatures on most nights were 10–13°C. Wind speeds were generally low (1–3 m s^{-1}) and wind direction was highly variable (Figure 1, middle). There were four periods of elevated wind speeds (2–4, 15–17, 20–21, and 26–28 January). Maximum wind speeds were attained on the morning of 3 January, reaching 14 m s^{-1}. Tidal height ranged from −1 to +2 m (Figure 1, bottom). Besides the diurnal and semidiurnal variations, there were significant weekly variations in tidal height.

2.3. Ancillary Measurements

[11] NO, NO_x, and O_3 were measured using Thermo-Electron Corp. models 42C and 49C, respectively. NO_x and O_3 data were recorded at 1-min intervals and averaged over 15 min periods. The data typically exhibit strong diurnal variations with daytime ozone maxima and nighttime NO_x maxima resulting from photochemical reactions, emissions, and surface losses. There are two anomalous periods (14–15 and 18–19 January) during which O_3 did not decrease at night and NO_x did not increase. The air masses associated with these two episodes arrived at the pier from the east after spending several days over land at an altitude ~650 mbar.

[12] Sulfur dioxide was monitored qualitatively as an indicator of when the instrument sampled ambient air and scrubbed ambient air. These measurements were made with the APCI/MS/MS using the $SO_5^- \rightarrow SO_3^-$ (112→80 amu) mass transition. The instrument was calibrated using an SO_2 permeation tube after the completion of the project.

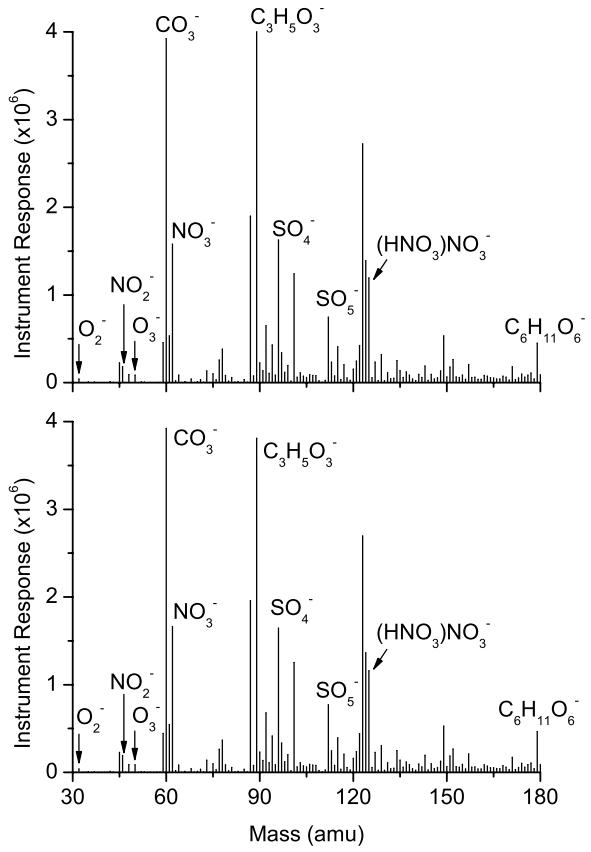

Figure 2. Ion spectra showing major ions in ambient air at Scripps Pier. Differences between major ions in the spectra are within ±3%. (top) 15 January with 40 ppb O_3, 5 ppb total NO_x, and 73% relative humidity. (bottom) 18 January with 5 ppb O_3, 25 ppb total NO_x, and 87% relative humidity.

The sensitivity of SO_2 to humidity and O_3 levels was not quantified.

3. Methods

3.1. Detection of Cl_2, Br_2, I_2, and Mixed Dihalogens

[13] The dihalogens Cl_2, Br_2, I_2, BrCl, ICl, and IBr were monitored using atmospheric pressure chemical ionization tandem mass spectrometry (APCI/MS/MS; Thermo Corporation TSQ Quantum). Negative ions were formed at atmospheric pressure by passing ambient air through a 1/4'' SS tube lined with a ^{63}Ni foil. The foil emits 67 keV that rapidly thermalize by collisions with O_2 and N_2. The primary negative ions formed are likely O_2^- and O_4^-, which rapidly cluster with water, giving $O_2^-(H_2O)_n$ and $O_4^-(H_2O)_n$ [*Siegel and Fite*, 1976]. These and other weakly electronegative transients undergo a variety of ion-molecule collisions reactions in the APCI source and 1 torr declustering region. The exact sequence of charge transfer reactions leading to the formation of dihalogen ions (e.g., Cl_2^-, Br_2^-, I_2^-) is not known.

[14] The dihalogens are considerably more electronegative than most common constituents of air. Some highly electronegative species such as NO_3 and CO_3 are formed in the source through ion molecule reactions. NO_2 has an electron affinity similar to that of Cl_2, and charge transfer can occur between either anion and the other neutral molecule [*Hughes et al.*, 1973]. These species compete for charge with the dihalogens and variations in their abundance have the potential to alter the instrumental response to dihalogens. Ambient air scans show NO_3^-, CO_3^-, and NO_2^- peaks (62, 60, and 46 amu, respectively) that are consistent in size, and do not vary with changes in ambient conditions such as NO_x levels, humidity, or temperature (Figure 2). This indicates that the abundance of these ions is primarily a function of ion-molecule chemistry in the ion source rather than ambient levels of precursors [*Finley*, 2007]. The insensitivity in major ions to ambient conditions likely explains why the sensitivity of the instrument to dihalogens is fairly constant. This is verified by standard additions of dihalogens to scrubbed ambient air and calibration curves in scrubbed air, as discussed below. It is important to note that the ion spectra observed in this instrument do not necessarily reflect their abundance in the ion source itself, but are modified by ion-molecule collisions during passage through the 1 torr region.

[15] Although halogen radicals exist in the ionization region, radical chemistry (e.g., Br + Br→Br_2) is unlikely to be a significant source of dihalogens. If radical chemistry were the source of the dihalogen signal (e.g., Br + CH_3Br→Br_2 + CH_3), we would expect to see similar dihalogen signals in both ambient air and in scrubbed ambient air (see section 3.2). In fact, dihalogen levels in scrubbed ambient air are usually <1% of the levels observed in ambient air. This result suggests that radical-mediated production of dihalogens is not a major contributor to the overall dihalogen signal.

[16] Once formed, the dihalogen ions were quadrupole mass filtered, then collisionally dissociated (1 mtorr Ar, 20 eV) into their constituent atoms (Cl^-, Br^-, and I^-), which were mass filtered in a second quadrupole. The ion transfer capillary between the APCI source and the mass spectrometer was maintained at 100°C.

[17] Chlorine and bromine each have two stable isotopes that yield four possible mass transitions for each molecular ion. Only one stable, naturally occurring isotope of iodine (^{127}I) exists resulting in a single transition for I_2. The dihalogen mass transitions monitored during this study are listed in Table 1. The mass spectrometer was run continuously except during periods of instrument calibration. Data was lost because of power outages on 11–12 and 14–15 January.

3.2. Sampling Inlet

[18] The air intake was located 2 m from the side of the pier and 10 m above the sea surface. Because dihalogen gases are surface reactive, a two-stage, laminar flow inlet was used to bring air to the instrument. The first stage consisted of approximately three meters of black 2'' ID ABS plastic pipe with PVC connectors. An airflow rate of 63 slpm was drawn through the pipe by a blower and monitored using a TSI 4216 flow sensor (TSI Corp.). The second stage consisted of a 1/2'' OD PFA Teflon tube that sampled 2.25 slpm isokinetically from the center of the first stage airflow using a vacuum pump and mass flow controller. Air was drawn from the central portion of this flow into the 1/4'' SS tube that contained the ^{63}Ni foil in the APCI

Table 1. Mass Transitions Used to Monitor Dihalogen Compounds in Air[a]

Dihalogen	Mass Transitions Monitored
Cl_2	$^{35}Cl^{35}Cl \rightarrow {}^{35}Cl$ (70→35)
	$^{35}Cl^{37}Cl \rightarrow {}^{35}Cl$ (72→35)*
	$^{35}Cl^{37}Cl \rightarrow {}^{37}Cl$ (72→37)
	$^{37}Cl^{37}Cl \rightarrow {}^{37}Cl$ (74→37)
Br_2	$^{79}Br^{79}Br \rightarrow {}^{79}Br$ (158→79)
	$^{79}Br^{81}Br \rightarrow {}^{79}Br$ (160→79)
	$^{79}Br^{81}Br \rightarrow {}^{81}Br$ (160→81)
	$^{81}Br^{81}Br \rightarrow {}^{81}Br$ (162→81)*
I_2	$^{127}I^{127}I \rightarrow {}^{127}I$ (254→127)*
BrCl	$^{79}Br^{35}Cl \rightarrow {}^{35}Cl$ (114→35)
	$^{81}Br^{35}Cl \rightarrow {}^{35}Cl$ (116→35)*
	$^{81}Br^{37}Cl \rightarrow {}^{35}Cl$ (118→37)
ICl	$^{35}Cl^{127}I \rightarrow {}^{35}Cl$ (162→35)*
	$^{37}Cl^{127}I \rightarrow {}^{37}Cl$ (164→37)
IBr	$^{79}Br^{127}I \rightarrow {}^{79}Br$ (206→79)*
	$^{81}Br^{127}I \rightarrow {}^{81}Br$ (208→81)

[a]The transitions used for quantitation are marked with an asterisk.

ionization source. This flow rate was 1 slpm and was controlled by the capillary ion transfer tube and the vacuum in the mass spectrometer. The flow rates were selected to maintain laminar flow and uniform linear flow rates across the inlet. The linear velocity of the gas was maintained at 0.5 m s^{-1}, resulting in a residence time of about 6 s. The inlet had a passing efficiency of 90 ± 11% for Cl_2, 91 ± 12% for Br_2, and 87 ± 12% for I_2. Passing efficiencies were determined using standard additions to scrubbed ambient air.

[19] The inlet had two air intakes, connected by a 2" ID tee. The "straight-through" side of the tee allowed sampling of ambient air, and the "right angle" side admitted ambient air through a 0.5 m length of black ABS pipe filled with a carbonate-coated glass wool scrubber. The scrubber was prepared by soaking glass wool in a 1% (w/w) solution of Na_2CO_3 and Milli-Q water for 1 h and allowing it to dry. The treated fiberglass wool was >99% effective at removing dihalogens from the air stream. Two pneumatically controlled gate valves were used to alternate between ambient and carbonate-scrubbed air. Aerosols were not intentionally removed from the sampled air stream. Instrument blank signals in a clean inlet were compared to blank signals in an inlet that was exposed to ambient air and sea salt aerosols for periods of 48 h and one week, respectively. The exposed inlets did not show significantly different blank levels or dihalogen response compared to the clean inlet, suggesting that accumulation of sea salt on inlet surfaces was not a significant source of interference.

3.3. Standards

[20] Cl_2, Br_2, and I_2 standards were generated using permeation tubes (VICI Metronics) stored under nitrogen in a temperature-controlled environment. The Cl_2 and Br_2 tubes were maintained at 30 ± 1°C and the I_2 tube was maintained at 100 ± 1°C. Weight records for these tubes were maintained before and after the experiment, with consistent results. As pointed out by *Keene et al.* [1993], the weight loss record of Cl_2 permeation tubes may not reflect the actual emission rate, presumably because of chemical reactions either in the tubes or on the outer surfaces of the tubes. To validate the permeation rates, the output of each of the permeation tubes was bubbled through a neutral KI solution (2% w/w KI, 1 mM phosphate buffer, pH = 7), in which dihalogens oxidized I^- to I_3^-. The absorption of I_3^- at 352 nm was measured with an Ocean Optics SR2000 spectrophotometer and a Xe lamp. The rate of halogen release from the permeation tubes was calculated from the rate of change of I_3^- absorbance, and the molar absorptivity of I_3^- (ε = 23,200 L mol^{-1} cm^{-1}) [*Wei et al.*, 2005]. The emission rates were consistently lower than the rates obtained from weight loss. The correction factors for the emission rates were 0.75 for Cl_2, 0.51 for Br_2, and 0.91 for I_2.

[21] Gas standards were added to the instrument inlet just after the 2" ID tee for 15 min every 4 h to check instrument sensitivity. The standards were generated at ppb levels from the permeation sources using a two-stage dilution system [*Gallagher et al.*, 1997]. A high-purity N_2 stream of 85 cm^3 min^{-1} was passed over the permeation device. A variable percentage of the flow (40–73%) was then dumped to waste. The remaining flow was diluted with a clean nitrogen stream and a second dump was used to vary the diluted flow. The dilution system flow was then added to the 63 slpm flow in the 2" ID pipe, reducing the ppb levels generated in the dilution system down to ppt levels.

[22] This approach has two advantages for calibration of reactive gases. First, the dihalogen standard contacts only PFA tubing and fittings, minimizing loss through surface reactions. Second, the range of different mixing ratios in the sampled air stream is generated by varying the flow rate of the standard delivered into the air inlet, while the mixing ratio of dihalogen in the tubing used to deliver the standard does not change. This avoids having to reequilibrate the tubing walls during calibration.

[23] Primary standards were not available for the mixed halogens BrCl, ICl, or IBr. Laboratory experiments to determine the instrument sensitivity to BrCl were carried out following the field study, as described in more detail below. Mixing ratios of ICl and IBr were estimated using the averaged Br_2 calibration curve.

3.4. Blanks and Interferences

[24] The inlet gate valves were programmed to periodically direct carbonate-scrubbed air through the inlet. The dihalogen levels measured during these periods are considered system "blanks," which are subtracted from the ambient dihalogen signals. The "blank" air contains many of the unreactive constituents of air such as O_2, N_2, most hydrocarbons, and halocarbons such as CFCs, HCFCs, methyl halides, etc. The scrubber should remove acidic constituents of air such as HCl, HNO_3, SO_2, and organic acids. This method of determining the system blank is not foolproof, but it should account for many potential interferences. To successfully generate a positive artifact in the system, an interfering molecule would need to (1) be removed by the carbonate scrubber and (2) form a dihalogen in the source either through neutral chemistry or ion-molecule interactions. Possible interferents are molecules like dichloroacetic and trichloroacetic acid (breakdown products of tetrachloroethene and 1, 1, 1-trichloroethane, respectively) and NCl_3 (a by-product of water treatment). We have tested these gases in the laboratory and found that

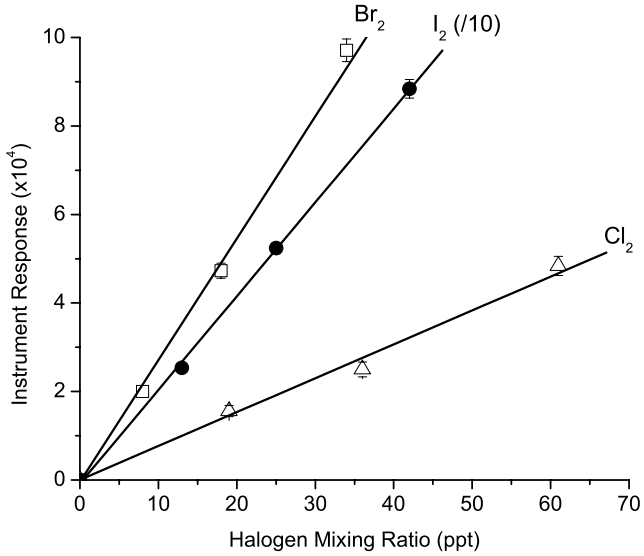

Figure 3. Calibration curves for Cl_2, Br_2, and I_2 from 5 January 2006. The I_2 calibration and standard errors were scaled down by a factor of 10 for convenient plotting. Uncertainties are one geometric standard error (n = 75). The curves show a linear response over the expected range of ambient mixing ratios. Solid circles, I_2; open squares, Br_2; open triangles, Cl_2.

they produce no Cl_2 response in the instrument. HCl does not produce Cl_2 signal.

3.5. Calibrations and Detection Limits

[25] Instrument calibrations consisted of adding varying levels of Cl_2, Br_2, and I_2 gas standards, ranging from 4 to 61 ppt, to blank air for 5 min at each level (Figure 3). Calibration curves were obtained from a linear least squares fit to the data. For all calibrations, there was a small negative intercept which may indicate the presence of a zero-order loss in the sampling system or ion source.

[26] Calibration for BrCl was done using a permeation device constructed in the laboratory. The permeation cell was a cylindrical 350 cm^3 PFA Teflon chamber with a radius of 5.4 cm and a height of 3.8 cm and Viton o-ring sealed flanges. A 60 cm length of 1/16" OD PTFE Teflon tubing (0.016" wall thickness) was passed into and out of the chamber via PFA compression feed-throughs. The chamber was maintained at 30°C with an 85 cm^3 min^{-1} flow of N_2. The permeation cell was flushed and filled with either 1% Cl_2 in zero air (1% Cl_2, AirGas), 1% Br_2 (99.5% Br_2 liquid, Fisher Scientific) in N_2, or a mixture of both. The emission rates of Br_2 and Cl_2 into the tubing were determined by filling the chamber with 1% Cl_2 or 1% Br_2 and comparing the output with gas streams from the commercial permeation sources described earlier. BrCl was generated by filling the chamber with a mixture of 1% Cl_2 and 1% Br_2 and allowing it to react for 24 h.

[27] BrCl, Cl_2, and Br_2 emitted from the permeation chamber were measured with the APCI/MS/MS. The permeation rate for BrCl was determined from the decrease in Cl_2 and Br_2 signals relative to the signals when the chamber was filled with each compound individually. The BrCl permeation rate was used in conjunction with the observed BrCl signal to estimate the sensitivity of the instrument for BrCl. Five different mixing dilutions of BrCl from the chamber output were added to the instrument inlet to generate a calibration curve. The APCI/MS/MS sensitivity to BrCl is 25% higher than that for Cl_2, intermediate between Cl_2 and Br_2. As an independent check on this method, the calculated mixing ratios were used to calculate the equilibrium constant for BrCl in the Cl_2+Br_2 mixture. The K_{eq} calculated was 9.2 ± 0.3 which is consistent with the literature value of 9.1 [*Tellinghuisen*, 2003].

[28] Similar experiments have not yet been carried out for IBr and ICl. In this paper, the Br_2 calibration curve was applied to the IBr and ICl signals. Applying the Cl_2 or I_2 calibration curves to the mixed halogen signals would not substantively alter the interpretation of the results.

[29] The practical detection limit of the dihalogen analysis in air is imposed by the variability in the blank signal. Typical blank signals correspond to <1–5 ppt of dihalogen. The detection limit was estimated using the observed variability in the blank signal, the error in the blank interpolation (see section 3.6), and the error in the calibration curve slope. Detection limits were estimated at 1 ppt (S/N = 2) for the 72→35 Cl_2 transition, 0.5 ppt for the 162→81 Br_2 transition, and 0.2 ppt for the 254→127 I_2 transition. The detection limit is equivalent to approximately 1 ions s^{-1} for Cl_2, 14 ions s^{-1} for Br_2, and 47 ions s^{-1} for I_2.

3.6. Data Processing

[30] Data collection with the APCI/MS/MS consisted of monitoring each mass transition in Table 1 for 1 s sequentially from lowest to highest parent mass. The total cycle time was 17 s, including the dihalogen and SO_2 mass transitions. The inlet gate valves were cycled to provide a 15 min period of blank after each hour of ambient air sampling. The SO_2 signal clearly indicates the blank intervals due to its high signal to noise and effective removal by the carbonate scrubber. The SO_2 signal was used to validate the operation of the gate valves when the instrument was unattended. Because of minor misalignment, one of the gate valves occasionally failed to close fully. Periods of blank containing anomalously high SO_2 levels were removed from the data set. The samples immediately following these periods of contaminated blanks were removed as well, since it was impossible to know whether the sample valve had properly opened or if the sample was contaminated with scrubbed air.

[31] The raw ambient measurements were averaged over 15 min intervals and corrected for instrument blank. The blank for each sample was calculated by linearly interpolating between the blank before and after each sampling interval. These blanks were subtracted from the ambient signals. The blank-corrected signals were converted into a mixing ratio using the calibration curve. A single calibration curve was used for the entire measurement period. This calibration was obtained by averaging the 6 individual calibrations measured during the study. No systematic changes in calibration were observed during the study period, within the estimated uncertainties. For Cl_2, Br_2, and I_2, the 72→35, 162→81, and 254→127 mass transitions were used for quantification.

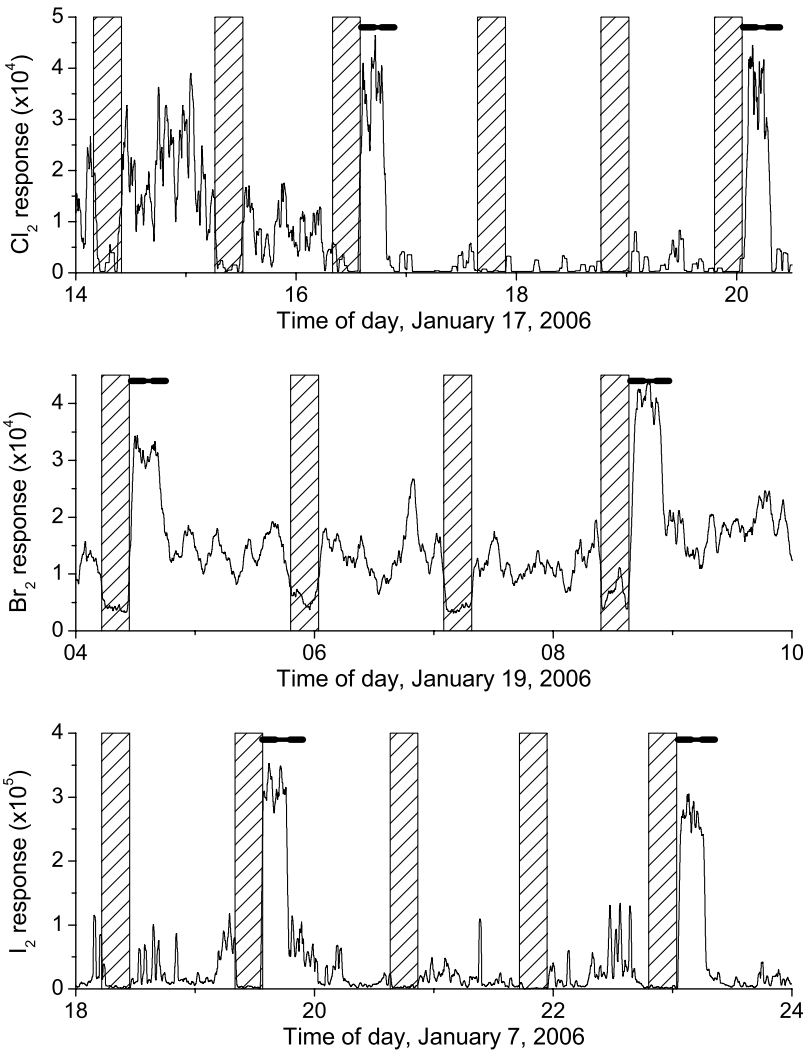

Figure 4. Raw instrument data for (top) Cl_2, (center) Br_2, and (bottom) I_2. Hatched areas show instrument blanks. Dark bars are placed over dihalogen gas standard additions. Standard additions were 20 ppt for Cl_2, 9 ppt for Br_2, and 15 ppt for I_2. Areas with no marking are ambient air.

[32] Raw data for Cl_2, Br_2, and I_2 is shown Figure 4. The ambient signal is considered below the instrument detection limit when the ambient signal cannot be distinguished from the blank signal. Standard additions to scrubbed ambient air are also shown.

[33] The uncertainties in the 15 min averaged mixing ratios were determined by propagating the lognormal variance in the raw 1 s data (as 1 geometric standard error of the mean), the uncertainty in the blank, and the uncertainty in the slope of the calibration curve. The resulting uncertainties ranged from ±0.1 to ±5 ppt. All means and uncertainties are reported as the geometric mean ± one geometric standard error of the mean. For computing mean dihalogen levels, data points below the detection limit were assumed to be 1/2 the detection limit.

4. Results and Discussion

4.1. Isotope Ratios

[34] Isotope ratios were examined as a test of the validity of the ambient dihalogen measurements. Because of large ambient variability and low ion counting rates, considerable time averaging was needed in order to reduce the uncertainty in the isotope ratios to useful levels. The ratios of various mass transitions were computed from the 15 min average blank-corrected ion currents. For Cl_2, these ratios were then averaged to compute a weekly average ratio for ambient air, standards, and blanks (Figure 5). The uncertainties in the ratios are reported as one standard error of the mean, calculated from the observed variances of the ratios. For ambient air and gas standards, only measurements above 4 ppt were used to compute isotope ratios.

[35] If the mass spectrometer signal at a parent mass of 72 is entirely due to $^{35}Cl^{37}Cl$, fragmentation should produce ion fragments at mass 35 and 37 with a ratio of 1. In the mass 72 signals from scrubbed air blanks, weekly average 72→35/72→ 37 ratios ranged from 0.23 to 0.32, with an overall mean of 0.28 ± 0.03 (n = 373) for the entire measurement period. This low isotope ratio suggests that the blank is due either to an unchlorinated compound, or to a molecule containing a single chlorine atom. This result suggests that the blank is not primarily Cl_2. The blank,

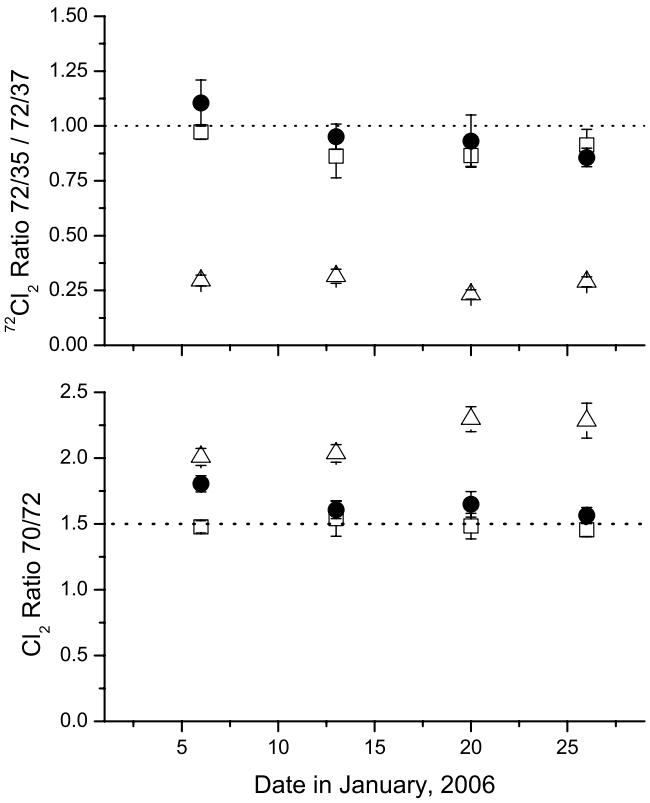

Figure 5. Weekly chlorine isotope ratios. (top) Ratio of 72→35/72→37 transitions for $^{72}Cl_2$. (bottom) Ratio of $^{70}Cl_2/^{72}Cl_2$. Solid circles, ambient air; open squares, gas standards; open triangles, scrubbed air blanks. The dotted line is the isotope ratio expected on the basis of the natural isotopic abundance of chlorine. Uncertainties are one standard error.

therefore, is not simply due to desorption of Cl_2 from the inlet walls or to the production of Cl_2 from aerosols that pass through the scrubber and reach the ion source. One possible candidate for the blank is $HOCl{\cdot}H_2O^-$. This singly chlorinated cluster would yield a 72→37 transition but would not give a corresponding 72→35 transition. Because HOCl is not be expected survive passage through the carbonate scrubber, it would need to be formed in the ion source. Cl_2 gas standards and ambient air exhibited 72→35/72→37 isotope ratios at mass 72 close to the expected value of 1.

[36] At the natural chlorine isotopic abundance, the ratio of $^{70}Cl_2$ ($^{35}Cl^{35}Cl$) to $^{72}Cl_2$ ($^{35}Cl^{37}Cl$) should be 1.5. This ratio was computed from the data by taking the ratio of the signal at the 70→35 transition to the sum of the 72→35 and 72→37 signals. The blanks have an average $^{70}Cl_2$:$^{72}Cl_2$ ratio of 2.2 ± 0.1 (n = 373) over the entire measurement period, with a range of 2.0 to 2.3. This is consistent with the presence of an $HOCl{\cdot}H_2O^-$ cluster, which would give a 70→35 transition as well as a 72→37 transition, and with the conclusion above that the blank is not primarily due to Cl_2. Cl_2 gas standards gave weekly average $^{70}Cl_2$:$^{72}Cl_2$ ratios ranging from 1.4 to 1.6 with an overall mean for the whole study of 1.5 ± 0.1 (n = 56). Weekly average ambient air ratios ranged from 1.55 to 1.8, with an overall mean $^{70}Cl_2$:$^{72}Cl_2$ ratio of 1.6 ± 0.2 (n = 236). During the first week of measurements, the $^{70}Cl_2$:$^{72}Cl_2$ ratio was slightly elevated, suggesting the presence of some interference in the at the 70→35 transition. Because the ratio of 72→35/72→37 does not show evidence of interference for standards or ambient air, the 72→35 transition was used to quantify ambient Cl_2 mixing ratios.

[37] Bromine isotope ratios (^{79}Br:^{81}Br) were also examined. Only Br_2 signals above 3 ppt were included in the ratio analysis for ambient air and gas standards. Ratios were computed from the 15 min average blank-corrected ion currents. The ratios were averaged over the full 27 day measurement period because of the very low ion statistics during the final week and the lack of regular standard additions during the first week. The uncertainty in the ratios is given as one standard error of the mean and is calculated from the observed variance of the ratios of the various bromine mass transitions.

[38] If the signal at mass 160 were composed entirely of Br_2, the ratio of 160→79/160→81 would be close to 1. The mean ratio of these transitions in blanks from this study was 0.78 ± 0.02 (n = 373). This ratio is slightly low, indicating that that at most, Br_2 can account for about 80% of the signal at mass 160. For the gas standards, the ratio was 1.0 ± 0.03 (n = 26) and for the ambient air the ratio was 0.94 ± 0.02 (n = 183). The results for the standards and ambient air are consistent with the signals originating primarily from Br_2.

[39] The isotope ratios of the parent bromine ions, $^{158}Br_2$:$^{160}Br_2$:$^{162}Br_2$ should be 0.5:1.0:0.5. This ratio was calculated for the field data by summing the 160→79 and 160→81 signals to calculate $^{160}Br_2$. The blank signals gave ratios of 0.46:1.0:0.45. This is consistent with the presence of some contamination of the $^{160}Br_2$ signal. The parent ratios for the Br_2 gas standards were 0.54:1.0:0.51 and ambient air gave ratios of 0.56:1.0:0.48. The uncertainty in these ratios ranged from 0.01 to 0.02 (1 se). Overall, the parent isotope ratios are consistent with the identity of the signal as predominantly due to Br_2, although the uncertainty in the ratios does not preclude minor contamination from other, possibly bromine-containing compounds. For quantifying the Br_2 signal, the 162→81 mass transition was chosen because it was the most consistent of the four transitions and showed the least evidence of interference.

4.2. Dihalogens and Large-Scale Meteorology

[40] Five-day air mass back trajectories at 250 m and 500 m were calculated at midnight, 0600, noon, and 1800 local time every day from 2 to 29 January. After generating the back trajectories, the trajectory cluster analysis function of the HYSPLIT v4.7 model was used to divide the trajectories into five distinct groups (Figure 6). Cl_2, Br_2, I_2, total NO_x, and O_3 ranges observed during each group are summarized in Table 2. The continental group consisted of air masses that spent 5 days over the U.S. and Canada. These air masses had 6 h or less of coastal influence before arriving at the site. The oceanic group was composed of air masses that spent 5 days over the Pacific Ocean with 12 h or less near the coast. The low-latitude group consisted of air masses originating over the Pacific Ocean from 30 to 33°N, the midlatitude group originated between 38 and 45°N, and the high-latitude group originated from 50 to 55°N. The

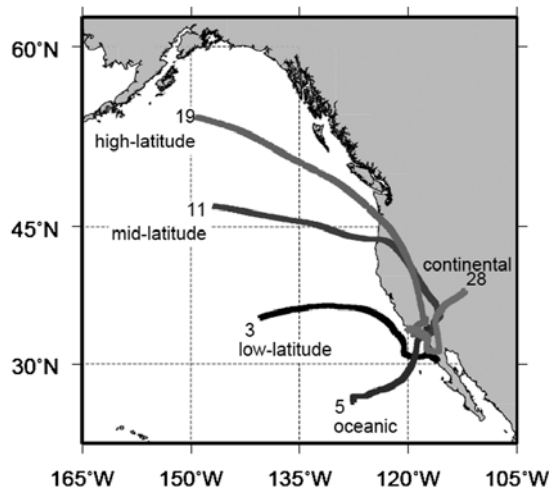

Figure 6. Sample 5-day 250 m air mass back trajectories from each air mass group. Back trajectories were run at midnight on the indicated date of January 2006 at 250 m.

low-, middle-, and high-latitude groups all originated over the Pacific Ocean, but spent at least 2–3 days over the U.S. west coast before arriving at the pier.

4.2.1. Dihalogens in the Continental Group

[41] The continental group of air masses consistently exhibited high levels of NO_x and O_3 due to the presence of strong anthropogenic sources. Cl_2 was regularly detectable in all of these air masses (Figure 7a). Typical Cl_2 levels were <5 ppt, but a 26 ppt maximum was observed around noon on 15 January. Typical Br_2 levels were <1 ppt except on 15 January when they reached 5.5 ppt (Figure 7b). I_2 in continental air was generally <0.5 ppt. On 27 January, I_2 increased from <0.1 ppt at 1500 local time to a maximum of 4 ppt near midnight (Figure 7c). These results suggest there may be a significant continental source of Cl_2 since it was regularly observed in continental air with no coastal influence. This source would most likely be anthropogenic, and related to use in swimming pools, cooling towers, and water treatment facilities. Br_2 and I_2 were only observed episodically, implying that continental sources may be less important for these compounds. The high I_2 mixing ratios on 27 January were observed in air masses that spent considerable time (4–6 h) over the coast. The source of the I_2 was most likely coastal, although anthropogenic sources cannot be ruled out.

4.2.2. Dihalogens in the Oceanic Group

[42] The oceanic air masses consistently showed the lowest levels of NO_x and O_3 (Table 2). Cl_2 levels in oceanic air were usually <5 ppt but were consistently above the detection limit (1 ppt) during the day. The highest Br_2 levels were observed in the oceanic group. Br_2 levels were typically <1 ppt but reached a daytime maximum of 9 ppt. The highest Br_2 mixing ratios in this group were observed during the day. Nighttime levels were lower (<0.5–2 ppt), although mixing ratios up to 5 ppt were observed after midnight on 16 January (Figure 7b). I_2 mixing ratios were consistently low in oceanic air, reaching a maximum of 1.5 ppt just before dawn on 5 January. Results from the oceanic group suggest a possible ocean/coastal source of Cl_2 and Br_2. This source is likely photochemical since the dihalogens were observed during the day, and the results are consistent with sea salt aerosol production of Cl_2 and Br_2. The oceanic group had up to 12 h of coastal influence before reaching the site, so the influence of anthropogenic pollutants (direct emissions or precursors) cannot be ruled out. The presence of I_2 in this group is consistent with a coastal source, most likely the scattered kelp beds near the coast.

4.2.3. Dihalogens in the Low-Latitude Group

[43] Low-latitude air masses (30–33°N) consistently showed low NO_x and O_3, except 5 January when NO_x reached 121 ppb. The large NO_x events in this group were likely caused by ship activity, since these air masses passed over the San Diego naval shipyard 16 km to the southeast. Dihalogens in this group were consistently above detection for Cl_2, Br_2, and I_2 (Figures 7a–7c). Cl_2 reached 21 ppt around 1300 local time on 6 January. Typical Cl_2 levels were between 2 and 4 ppt during the day, similar to those observed in continental air. Br_2 was typically 1–2 ppt, with a maximum of 9 ppt at noon on 6 January. This group showed the highest I_2 mixing ratios, reaching a peak of 4 ppt at 0400 local time on 3 January. The high I_2 levels in this group were likely due to the passage of the air masses over the large kelp beds in the bay to the southeast.

[44] Cl_2 and Br_2 variability was higher in the low-latitude group than any other group, with levels ranging from undetectable levels to several parts per trillion within a few hours. This suggests either a highly variable, fixed dihalogen source or a spatially heterogeneous source. The I_2 was also variable in these air masses and can probably be explained by the patchiness of the kelp beds.

4.2.4. Dihalogens in the Midlatitude Group

[45] The midlatitude group (38–45°N) had the highest average NO_x levels (usually 25–40 ppb) with O_3 mixing ratios similar to the continental and high-latitude groups. The air masses in this group originated over the ocean, moved down the west coast, and spent several days recirculating over the southern California coast. I_2 mixing ratios were generally <0.2 ppt. Br_2 levels were typically <1 ppt, but reached 5 ppt on 10 January (Figure 7b). Cl_2 mixing ratios were similar to continental and low-latitude air, ranging from <1–17 ppt.

Table 2. Five-Day Air Mass Back Trajectory Groups With Observed Dihalogen and Pollutant Ranges

Category	Date in January	Cl_2 (ppt)	Br_2 (ppt)	I_2 (ppt)	NO_x (ppb)	O_3 (ppb)
Continental	14–15, 26–29	<1–26	<0.5–6	<0.2–4.5	5–68	3–74
Oceanic	5,16–17	<1–8	<0.5–9	<0.2–1.5	3–22	2–40
Low latitude	3–4, 6–9	<1–21	<0.5–8	<0.2–4.5	5–121	2–47
Midlatitude	10–13, 18, 20–22, 24	<1–17	<0.5–6	<0.2–3.5	4–102	2–55
High latitude	19, 23, 25	<1–11	<0.5–5	<0.2–3.5	4–73	3–74

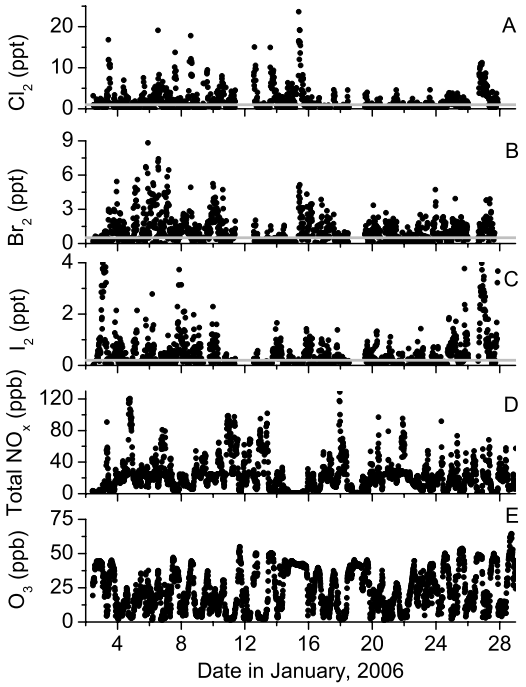

Figure 7. Mixing ratios for (a) Cl_2, (b) Br_2, (c) I_2, (d) total NO_x, and (e) O_3 observed at Scripps Pier from 2 to 29 January 2006. Points are 15 min averages. The dihalogen detection limits are shown as gray lines.

4.2.5. Dihalogens in the High-Latitude Group

[46] NO_x levels in the high-latitude air masses were similar to low-latitude and midlatitude air but had higher O_3 levels similar to continental air (Table 2). High pollutant levels were due to anthropogenic coastal sources. All of these air masses spent 2–3 days moving down the west coast and passed over Los Angeles, Orange, and northern San Diego counties. This group had the lowest dihalogen levels of any continentally influenced air masses. Cl_2 was usually <5 ppt and I_2 was <0.5 ppt. Br_2 levels were below 1 ppt most of the time. With minimal coastal influence in the 24–48 h prior to arriving at the site, sea salt aerosol Cl_2 and Br_2 sources were unlikely. The absence of large kelp beds north of the site probably explains the lack of I_2. The low dihalogen variability in these air masses may suggest that they were aged air masses that had lost dihalogens to photolysis and contained dehalogenated or very few sea salt aerosols.

4.3. Dihalogens and Local Meteorology

[47] Dihalogen mixing ratios are plotted as a function of wind speed and direction in Figure 8. Cl_2 was detectable at levels ranging from <1–28 ppt in winds from all directions (Figure 8). The highest Cl_2 levels (11–28 ppt) were observed in winds with speeds of 1–3 m s^{-1} with no directional preference and in winds from the southeast at 6–9 m s^{-1}. The detection of Cl_2 at low wind speeds during the day suggests a local Cl_2 source and is consistent with sea salt aerosol production, although local anthropogenic

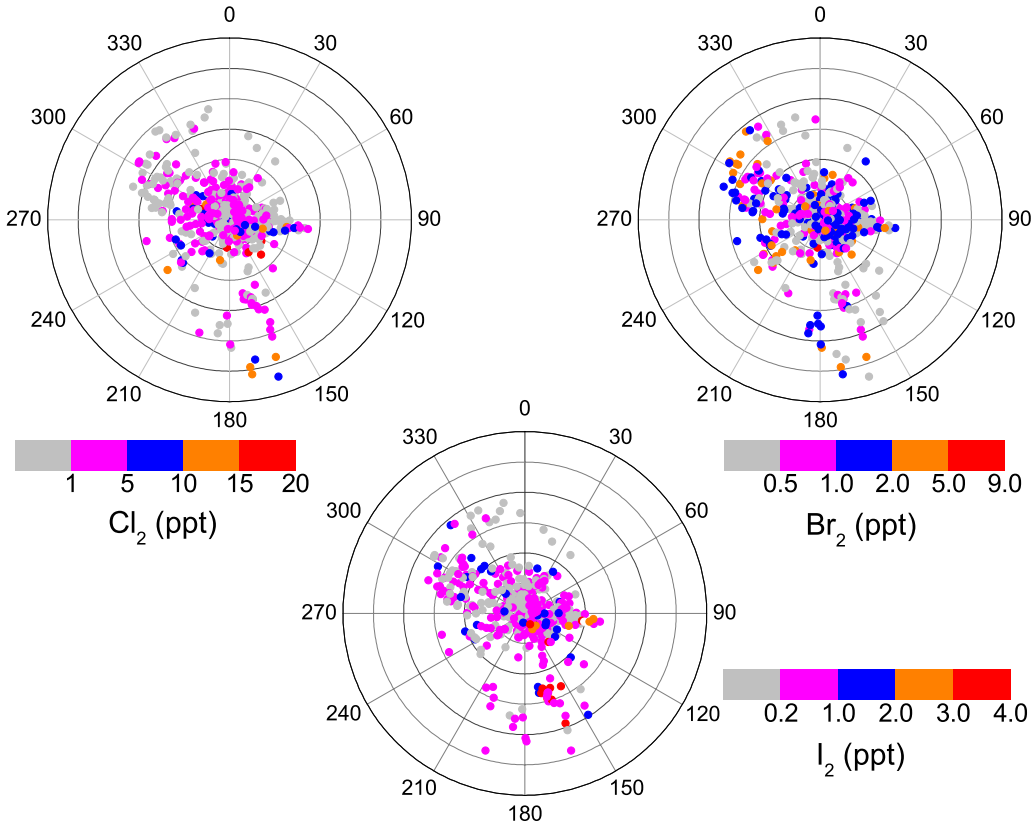

Figure 8. Wind roses for (top left) Cl_2, (top right) Br_2, and (bottom) I_2. Concentric rings represent wind speed, ranging from 0 m s^{-1} at the center to15 m s^{-1} at the outermost ring in increments of 2.5 m s^{-1} per ring. The pier is oriented northwest/southeast from the center along the 300° line.

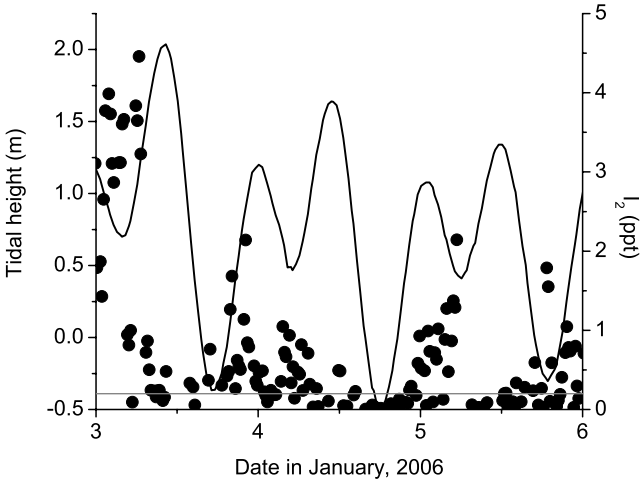

Figure 9. Tidal height (black line) and I_2 mixing ratio (circles) from 3 to 6 January 2006. The horizontal gray line is the I_2 detection limit.

sources (e.g., swimming pools, sprinkler systems) could not be ruled out.

[48] The highest levels of Br_2 (4–9 ppt) were consistently detected in daytime onshore winds from the northwest with speeds of 6–8 m s^{-1} (Figure 8). Elevated Br_2 mixing ratios in onshore air are consistent with a sea salt aerosol source of Br_2. Br_2 was detected at elevated wind speeds, which also suggests a sea salt aerosol source due to higher sea salt loads [see *Lewis and Schwartz*, 2004, Figure 22]. This may not be the only source, however, since Br_2 was detectable in winds from all directions, including offshore winds.

[49] Simultaneously high Br_2 and Cl_2 levels were observed in winds from the southeast on 6 and 15–16 January (Figure 8). On 7 and 27 January, Cl_2 was observed at levels of 5–10 ppt during periods of low wind speed (1–3 m s^{-1}) when Br_2 levels only reached 3 ppt. During these two cases (simultaneous Cl_2/Br_2 and primarily Cl_2) the observed NO_x and O_3 had similar ranges and mean levels. The similarity in the pollutant concentrations suggest that some additional source of variability, aerosol pH for example, is needed to explain these results.

[50] Maximum I_2 levels were observed in southeasterly winds at 6–9 m s^{-1}(Figure 8). That air was likely influenced by large local kelp beds, a known source of I_2 [*Palmer et al.*, 2005]. Other periods of increased wind speed either occurred during midday, when I_2 photolysis would prevent its transport to the sampling site, or did not pass over the kelp beds before reaching the pier. I_2 was detectable at low wind speeds (1–3 m s^{-1}) independent of direction, suggesting the presence of a source very close to the pier. The local source may be heterogeneously distributed patches of kelp. Offshore winds also showed detectable I_2, perhaps due to kelp and other seaweed washed up on the beach.

[51] Figure 9 shows that I_2 was not strongly correlated with tidal height. I_2 was observed during high tide and low tide. The highest I_2 mixing ratio of 4.5 ppt was observed during a period of high tide. The afternoon and evening of 3 January and the period from 2300 local time to sunrise on 4–5 January showed increasing I_2 levels even as the tide was rising. The rapid I_2 decreases from 0.6 to 0.9 ppt to near the detection limit on 3 and 5 January occurred at sunrise, when photolysis rapidly destroyed I_2.

4.4. Mean Dihalogen Levels

[52] Geometric mean dihalogen mixing ratios for the 27 days of observations were calculated using the 15-min averaged blank-corrected data (Figure 7a). For Cl_2, the mean level was 2.3 ± 1 ppt. Cl_2 was above the detection limit (1 ppt) for 55% of the 15 min measurement periods. The daytime mean Cl_2 level was 2.8 ± 1.0 ppt and the nighttime mean level was 1.5 ± 0.7 ppt.

[53] Br_2 in ambient air had a mean mixing ratio of 2.3 ± 0.4 ppt, well above the detection limit of 0.5 ppt (Figure 7b). Br_2 was detectable for 82% of the measurement intervals. Iodine ranged from below the detection limit of 0.2 ppt to a maximum of 4.5 ppt (Figure 7c). The mean I_2 mixing ratio for the entire month was 0.7 ± 0.1 ppt. 73% of the total I_2 measurements were above the detection limit.

4.5. Dihalogen Temporal Patterns

[54] Cl_2 levels >5 ppt occurred more frequently during the daytime than at night, supporting a photochemical production mechanism. There were 146 Cl_2 measurements greater than 5 ppt. 104 of these points were detected during the day and only 42 were detected at night. Figure 10 shows that Cl_2 was above the detection limit every day for several hours during the first week of measurements, reaching a maximum between noon and 1600 local time. At night, Cl_2 levels were close to the detection limit and consistently exceeded the detection limit only on 6–7 January. The data do not support a strong nighttime Cl_2 production mechanism. Cl_2 was regularly detectable during the first week of the study. The appearance of Cl_2 during the last three weeks was irregular, usually for an hour or two at a time.

[55] Br_2 was observed both day and night with no consistent diurnal cycle (Figure 10). Br_2 was detectable during the day on 3–10 January and during the night on 4–10 January. The ambient levels of Br_2 follow a pattern similar to Cl_2, with higher levels during the first week, and lower, more variable levels afterward (Figure 7). During the first week of measurements, Br_2 regularly reached levels of 1–4 ppt. At night, Br_2 usually appeared unaccompanied by Cl_2.

[56] The observed diurnal pattern of Br_2 requires daytime and nighttime production. The only known mechanisms that can account for nighttime Br_2 are surface reactions of O_3, $BrONO_2$, and $BrNO_2$ with aerosol Br^- [*Schweitzer et al.*, 1998; *Sander et al.*, 1999; *Hunt et al.*, 2004]. Proposed daytime production mechanisms for Br_2 include bulk aerosol/gas phase autocatalytic cycles and surface reactions of OH and Br^- [*Fan and Jacob*, 1992; *Vogt et al.*, 1996; *Frinak and Abbatt*, 2006]. The episodic nature of the Br_2 signals observed in this study suggests that variations in aerosol chemistry may play a dominant role in the production of Br_2. Future field studies involving simultaneous Br_2 and aerosol chemistry measurements are needed to rigorously test hypotheses for Br_2 formation.

[57] I_2 exhibited strong diurnal variability. During the first week, nighttime levels were 1–3 ppt higher than daytime levels (Figure 10). For the last three weeks, the difference between night and day was usually 0.2–0.5 ppt.

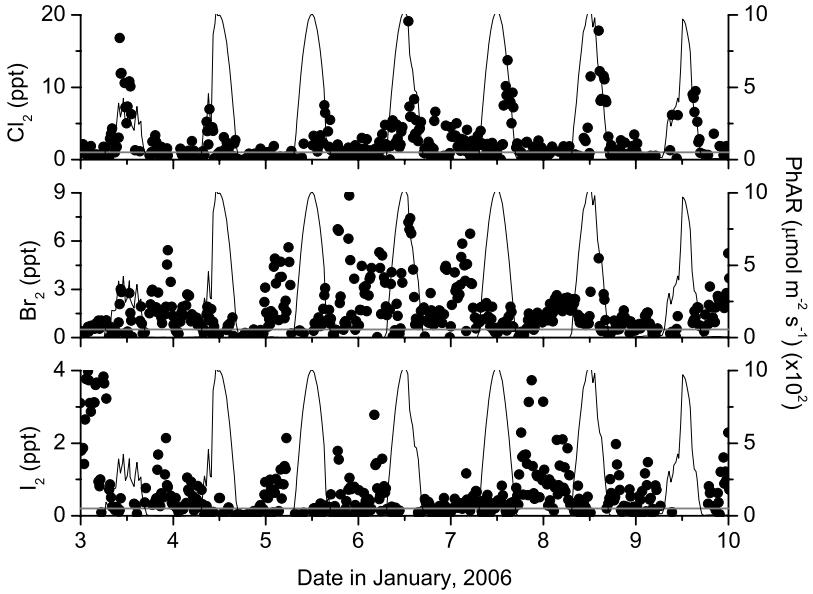

Figure 10. Measurements from 3 to 10 January 2006 from Scripps Pier illustrating the diurnal variability of (top) Cl_2, (center) Br_2, and (bottom) I_2. Solar flux, as photosynthetically active radiation, is also shown (solid black line). The horizontal gray line is the dihalogen detection limit.

Daytime I_2 reached a maximum of 3 ppt on the afternoon of 26 January. Overall, I_2 levels were highest during the first week of the study. The final 2 days of measurements also showed I_2 levels up to 4.5 ppt. When I_2 was detectable during the day, it was observed between 0800 and 1000 local time and from 1400 local time until sunset. I_2 was rarely detectable around noon. Daytime I_2 mixing ratios around noon ranged from <0.2–0.5 ppt. The source of the daytime I_2 was likely very close to the pier. The very short photolysis lifetime (~5 s) prevents transport of I_2 to the site.

[58] Nighttime I_2 levels are strongly influenced by NO_3. NO_3 reacts rapidly with I_2 ($k = 1.5 \times 10^{-12}$ cm^3 molecule^{-1} s^{-1}) [*Chambers et al.*, 1992] to form $IONO_2$ and I atoms. NO_3 levels at the pier were estimated to be 12 ppt using a photochemical box model and the NO_x and O_3 levels measured at the pier. Twelve ppt of NO_3 gives an I_2 lifetime of 37 min. It would take 30–50 min for I_2 from the kelp beds to the southeast to reach the pier at the typical 1–2 m s^{-1} wind speeds observed. This suggests that when NO_3 levels were ~10 ppt or higher, I_2 may not reach the sampling site before being destroyed by NO_3.

4.6. Mixed Halogens

[59] The mixed halogens BrCl, ICl, and IBr were never observed above their detection limits, estimated at 0.5 ppt, 0.5 ppt, and 0.4 ppt, respectively. The two transitions monitored for ICl and the two monitored for IBr were indistinguishable from the blank during the entire period. The three mass transitions monitored for BrCl were never distinguishable from the blank. These results imply that there was not a detectable source of the mixed halogens from production via sea salt aerosols. Gas phase production of mixed halogens from ClO+BrO should be insignificant at the levels of Cl_2, Br_2, and I_2 observed. Other sources, such as Cl + Br_2, were also expected to be negligible since halogen atoms were more likely to react with NO_x, hydrocarbons, or O_3 than with other dihalogens.

4.7. Comparison With Previous Measurements

[60] The Cl_2 levels observed in this study are consistent with other measurements of Cl_2. Table 3 compares our results with several other field observations of Cl_2. While most of our results are below the detection limits of the previous work, there is overlap in the observed ranges from 15 to 30 ppt. The very high levels (>100 ppt) reported by *Spicer et al.* [1998] or *Keene et al.* [1993] were not observed.

[61] The Br_2 measurements here are, to the best of our knowledge, the first reported in the coastal marine boundary layer so there is no basis for comparison with previous

Table 3. Summary of Published Measurements of Reactive Chlorines Species in Marine Air[a]

Location	Species	Range (ppt)	Methodology	Reference
Miami, FL	Cl*	<13 to 127	tandem mist chamber	*Keene et al.* [1993]
Bermuda	Cl*	<15 to 129	tandem mist chamber	*Keene and Savoie* [1996]
Long Island, NY	Cl_2	<16 to 150	APCI/MS/MS	*Spicer et al.* [1998]
Hawaii	Cl*	<13 to 24	tandem mist chamber	*Pszenny et al.* [2004]
Irvine, CA	Cl_2	<3.5 to 20	APCI/MS/MS	*Finley and Saltzman* [2006]
La Jolla, CA	Cl_2	<3 to 28	APCI/MS/MS	this study

[a]The tandem mist chamber measures Cl* as Cl_2 plus a small contribution from HOCl. These reported ranges assume all of the Cl* is Cl_2.

Table 4. Lifetimes of Elemental Mercury With Respect to Oxidation by OH, Br, and Cl, Based on the Mean Dihalogen Levels Observed During This Study[a]

	OH	Br	Cl
Concentration (cm^{-3})	1.2×10^5	6.1×10^4	7.7×10^3
Hg^0 lifetime (days)	964[b]	59[c]	150[d]

[a]Radical concentrations are 24 h means, estimated using a photochemical box model [*Finley*, 2007].
[b]$k = 10^{-13}$ [*Raofie and Ariya*, 2003].
[c]$k = 3.2 \times 10^{-12}$ [*Ariya et al.*, 2002].
[d]$k = 1 \times 10^{-11}$ [*Ariya et al.*, 2002].

work. These are the first I_2 measurements using APCI/MS/MS in coastal urban air. At Mace Head, Ireland, I_2 correlated with tidal height, suggesting that emissions were associated with exposure of nearby macroalgae [*Saiz-Lopez and Plane*, 2004]. The I_2 signal at Scripps Pier does not show a significant relationship with tidal height (Figure 8), although the tidal range at the two sites is similar (3 m). The lack of I_2 correlation with tidal height may be due to the absence of exposed macroalgae near the pier.

4.8. Implications of Observed Dihalogen Levels

[62] The Cl_2 levels observed at Scripps Pier suggest that chlorine chemistry can have a significant influence on O_3 levels in polluted coastal air. Photochemical box model simulations of similar Cl_2 levels at Irvine, California suggested that up to 10% of the observed O_3 during this study may be attributable to production by chlorine atoms [*Finley and Saltzman*, 2006; *Finley*, 2007]. Those results were consistent with previous model studies of halogen-mediated O_3 formation in polluted air [*Knipping and Dabdub*, 2003].

[63] Halogen atoms generated from the photolysis of Br_2 and Cl_2 can also affect the conversion of airborne elemental mercury to reactive gaseous mercury. A photochemical box model was used to estimate the levels of Cl and Br atoms resulting from the Br_2 and Cl_2 measured during this study [*Finley*, 2007; *Yvon et al.*, 1996]. At these levels, the atmospheric lifetime of elemental mercury (Hg^0) is estimated to be 59 days with respect to Br atoms and 150 days with respect to Cl atoms (Table 4). The combined lifetime of 42 days is considerably shorter than the global mean lifetime of 6–24 months [*Schroeder and Munthe*, 1998]. This suggests that conversion of mercury may be enhanced in coastal urban environments, and that polluted air advected over the oceans may have an impact on the global lifetime of elemental mercury.

5. Conclusions

[64] This study demonstrates low parts per trillions detection of dihalogens in air using APCI/MS/MS. The detection limit of the technique is controlled by the variability in the blank signal in carbonate-scrubbed air. The origin of this blank signal is not yet fully understood. The detection limits of the technique may be improved through better characterization and control of the instrument blank.

[65] The dihalogens Cl_2, Br_2, and I_2 were present at significant and highly variable levels in polluted coastal air. The halogen atoms resulting from the photolysis of Cl_2 cause a net production of ozone, while those from Br_2 and I_2 destroy ozone. The observed dihalogen levels place a lower bound on the possible importance of halogen chemistry, as there may be other precursors of halogen atoms that do not involve dihalogens. An example is the reaction of OH + HCl. This reaction has been shown to be important when HCl levels are >1 ppb [*Keene et al.*, 2007]. Measurements of halogen reservoir species like HOCl or $ClONO_2$ are needed to assess the full extent of halogen photochemistry in tropospheric air. This study suggests that dihalogen chemistry may play a role in coastal urban air quality. Further study is needed to assess the spatial and temporal extent of dihalogens and fully understand their origin, fate, and impact.

[66] **Acknowledgments.** The authors wish to acknowledge John Greaves for analytical advice and Cyril McCormick for engineering assistance. The authors thank Brad Hart and Alan Schoen of Thermo Corporation for their support and technical advice. The authors benefited from scientific discussion with Mike Lawler, Olga Pikelnaya, Jochen Stutz, John Plane, Alfonso Saiz-Lopez, and Roland von Glasow. The authors thank the Scripps Institute of Oceanography for use of the pier, Christian McDonald for logistical support, Ed Parnell for a kelp bed map, and reviewers for helpful criticism and comments. This research was supported by the National Science Foundation under grant ATM-0614816 and is a contribution to U.S. SOLAS.

References

Alicke, B., K. Hebestreit, J. Stutz, and U. Platt (1999), Iodine oxide in the marine boundary layer, *Nature*, *397*, 572–573, doi:10.1038/17508.

Allan, B. J., G. McFiggans, J. M. C. Plane, and H. Coe (2000), Observation of iodine oxide in the remote marine boundary layer, *J. Geophys. Res.*, *105*, 14,363–14,370, doi:10.1029/1999JD901188.

Ariya, P. A., A. Khalizov, and A. Gidas (2002), Reactions of gaseous mercury with atomic and molecular halogens: Kinetics, products studies, and atmospheric implications, *J. Phys. Chem.*, *106*, 7310–7320.

Ayers, G. P., R. W. Gillett, J. M. Cainey, and A. L. Dick (1999), Chloride and bromide loss from seasalt particles in Southern Ocean air, *J. Atmos. Chem.*, *33*, 299–319, doi:10.1023/A:1006120205159.

Behnke, W., C. George, V. Scheer, and C. Zetzsch (1997), Production and decay of $ClNO_2$ from the reaction of gaseous N_2O_5 with NaCl solution: Bulk and aerosol experiments, *J. Geophys. Res.*, *102*, 3795–3804, doi:10.1029/96JD03057.

Carpenter, L. J., W. T. Sturges, S. A. Penkett, P. S. Liss, B. Alicke, K. Hebestreit, and U. Platt (1999), Short-lived alkyl iodides and bromides at Mace Head, Ireland: Links to biogenic sources and halogen oxide production, *J. Geophys. Res.*, *104*, 1679–1689, doi:10.1029/98JD02746.

Carpenter, L. J., K. Hebestreit, U. Platt, and P. S. Liss (2001), Coastal zone production of IO precursors: A 2-dimensional study, *Atmos. Chem. Phys.*, *1*, 9–18.

Chambers, R. M., A. C. Heard, and R. P. Wayne (1992), Inorganic gas-phase reactions of the nitrate radical: $I_2 + NO_3$ and $I + NO_3$, *J. Phys. Chem.*, *96*, 3321–3331, doi:10.1021/j100187a028.

Chang, S., E. McDonald-Buller, Y. Kimura, G. Yarwood, J. Neece, M. Russell, P. Tanaka, and D. Allen (2002), Sensitivity of urban ozone formation to chlorine emission estimates, *Atmos. Environ.*, *36*, 4991–5003, doi:10.1016/S1352-2310(02)00573-3.

Davis, D., J. Crawford, S. Liu, S. McKeen, A. Bandy, D. Thornton, F. Rowland, and D. Blake (1996), Potential impact of iodine on tropospheric levels of ozone and other critical oxidants, *J. Geophys. Res.*, *101*, 2135–2147, doi:10.1029/95JD02727.

Dickerson, R. R., K. P. Rhoads, T. P. Carsey, S. J. Oltmans, J. P. Burrows, and P. J. Crutzen (1999), Ozone in the remote marine boundary layer: A possible role for halogens, *J. Geophys. Res.*, *104*, 21,385–21,395, doi:10.1029/1999JD900023.

Draxler, R. R., and G. D. Hess (1997), Description of the HYSPLIT_4 modeling system, *Tech. Memo. ERL ARL-224*, NOAA, Silver Spring, Md.

Draxler, R. R., and G. D. Hess (1998), An overview of the HYSPLIT_4 modeling system for trajectories, dispersion and deposition, *Aust. Meteorol. Mag.*, *47*, 295–308.

Eriksson, E. (1959a), The yearly circulation of chloride and sulfur in nature; meteorological, geochemical, and pedagogical implications: Part I, *Tellus*, *11*, 375–403.

Eriksson, E. (1959b), The yearly circulation of chloride and sulfur in nature; meteorological, geochemical, and pedagogical implications: Part II, *Tellus*, *12*, 63–109.

Fan, S.-M., and D. J. Jacob (1992), Surface ozone depletion in Arctic spring sustained by bromine reactions on aerosols, *Nature*, *359*, 522–524, doi:10.1038/359522a0.

Finlayson-Pitts, B. J., and J. C. Hemminger (2000), Physical chemistry of airborne sea salt particles and their components, *J. Phys. Chem. A*, *104*, 11,463–11,477, doi:10.1021/jp002968n.

Finley, B. D. (2007), Detection of dihalogens in coastal urban air, Ph.D. thesis, Univ. of Calif., Irvine.

Finley, B. D., and E. S. Saltzman (2006), Measurement of Cl_2 in coastal urban air, *Geophys. Res. Lett.*, *33*, L11809, doi:10.1029/2006GL025799.

Frinak, E. K., and J. P. D. Abbatt (2006), Br_2 production from the heterogeneous reaction of gas-phase OH with aqueous salt solutions: Impacts of acidity, halide concentrations, and organic surfactants, *J. Phys. Chem. A*, *110*, 10,456–10,464, doi:10.1021/jp063165o.

Gallagher, M. S., D. B. King, P.-Y. Whung, and E. S. Saltzman (1997), Performance of the HPLC/fluorescence SO_2 detector during the GASIE instrument intercomparison experiment, *J. Geophys. Res.*, *102*, 16,247–16,254, doi:10.1029/97JD00700.

Hedgecock, I. M., N. Pirrone, F. Sprovieri, and E. Pesenti (2003), Reactive gaseous mercury in the marine boundary layer: Modeling and experimental evidence of its formation in the Mediterranean region, *Atmos. Environ.*, *37*, suppl. 1, 41–49, doi:10.1016/S1352-2310(03)00236-X.

Holmes, C. D., D. J. Jacob, and X. Yang (2006), Global lifetime of elemental mercury against oxidation by atomic bromine in the free troposphere, *Geophys. Res. Lett.*, *33*, L20808, doi:10.1029/2006GL027176.

Honninger, G., H. Leser, O. Sebastian, and U. Platt (2004), Ground-based measurements of halogen oxides at the Hudson Bay by longpath DOAS and passive MAX-DOAS, *Geophys. Res. Lett.*, *31*, L04111, doi:10.1029/2003GL018982.

Hughes, B. M., C. Lifshitz, and T. O. Tiernan (1973), Electron affinities from endothermic negative-ion charge-transfer reactions. III. NO, NO_2, SO_2, CS_2, Cl_2, Br_2, I_2, and C_2H^*, *J. Chem. Phys.*, *59*(6), 3162–3181, doi:10.1063/1.1680458.

Hunt, S. W., M. Roeselavá, W. Wang, L. M. Wingen, E. M. Knipping, D. J. Tobias, D. Dabdub, and B. J. Finlayson-Pitts (2004), Formation of molecular bromine from the reaction of ozone with deliquesced NaBr aerosol: Evidence for interface chemistry, *J. Phys. Chem. A*, *108*, 11,559–11,572, doi:10.1021/jp0467346.

Johansen, A. M., R. L. Siefert, and M. R. Hoffmann (2000), Chemical composition of aerosols collected over the tropical North Atlantic Ocean, *J. Geophys. Res.*, *105*, 15,277–15,312, doi:10.1029/2000JD900024.

Keene, W. C., and D. L. Savoie (1996), The pH of deliquesced sea-salt aerosol in polluted marine air, *Geophys. Res. Lett.*, *25*, 2181–2194.

Keene, W. C., J. R. Maben, A. A. P. Pszenny, and J. N. Galloway (1993), Measurement technique for inorganic chlorine gases in the marine boundary layer, *Environ. Sci. Technol.*, *27*, 866–874, doi:10.1021/es00042a008.

Keene, W. C., R. Sander, A. A. P. Pszenny, R. Vogt, P. J. Crutzen, and J. N. Galloway (1998), Aerosol pH in the marine boundary layer: A review and model evaluation, *J. Aerosol Sci.*, *29*, 339–356, doi:10.1016/S0021-8502(97)10011-8.

Keene, W. C., et al. (2007), Chemical and physical characteristics of nascent aerosols produced by bursting bubbles at a model air-sea interface, *J. Geophys. Res.*, *112*, D21202, doi:10.1029/2007JD008464.

Knipping, E. M., and D. Dabdub (2002a), Modeling Cl_2 formation from aqueous NaCl particles: Evidence for interfacial reactions and importance of Cl_2 decomposition in alkaline solution, *J. Geophys. Res.*, *107*(D18), 4360, doi:10.1029/2001JD000867.

Knipping, E. M., and D. Dabdub (2002b), Chlorine emissions from activated seasalt aerosols and their potential impact on ozone, final report, Calif. Air Resour. Board, Sacramento, Calif.

Knipping, E. M., and D. Dabdub (2003), Impact of chlorine emissions from seasalt aerosol on coastal urban ozone, *Environ. Sci. Technol.*, *37*, 275–284, doi:10.1021/es025793z.

Knipping, E. M., M. J. Lakin, K. L. Foster, P. Jungwirth, D. J. Tobias, R. B. Gerber, D. Dabdub, and B. J. Finlayson-Pitts (2000), Experiments and molecular/kinetics simulations of ion-enhanced interfacial chemistry on aqueous NaCl aerosols, *Science*, *288*, 301–306, doi:10.1126/science.288.5464.301.

Kupper, F. C., N. Schweigert, E. A. Gall, J. M. Legendre, H. Vilter, and B. Kloareg (1998), Iodine uptake in Laminariales involves extracellular haloperoxidase-mediated oxidation of iodide, *Planta*, *207*, 162–171.

Laurier, F. J. G., R. P. Mason, L. Whalin, and S. Kato (2003), Reactive gaseous mercury formation in the North Pacific Ocean's marine boundary layer: A potential role of halogen chemistry, *J. Geophys. Res.*, *108*(D17), 4529, doi:10.1029/2003JD003625.

Leser, H., G. Honninger, and U. Platt (2003), MAX-DOAS measurements of BrO and NO_2 in the marine boundary layer, *Geophys. Res. Lett.*, *30*(10), 1537, doi:10.1029/2002GL015811.

Lewis, E. R., and S. E. Schwartz (2004), *Sea Salt Aerosol Production: Mechanisms, Methods, Measurements and Models: A Critical Review*, *Geophys. Monogr. Ser.*, vol. 152, edited by E. R. Lewis and S. E. Schwartz, AGU, Washington, D. C.

Nightingale, P. D., G. Malin, and P. S. Liss (1995), Production of chloroform and other low-molecular-weight halocarbons by some species of macroalgae, *Limnol. Oceanogr.*, *40*, 680–689.

O'Dowd, C. D., J. L. Jimenez, R. Bahreini, R. C. Flagan, J. H. Seinfeld, K. Hämeri, L. Pirjola, M. Kulmala, S. G. Jennings, and T. Hoffmann (2002), Marine particle formation by biogenic iodine emissions, *Nature*, *417*, 632–636, doi:10.1038/nature00775.

Oum, K., M. J. Lakin, D. O. D. Haan, T. Brauers, and B. J. Finlayson-Pitts (1998), Formation of molecular chlorine from the photolysis of ozone and aqueous seasalt particles, *Science*, *279*, 74–77, doi:10.1126/science.279.5347.74.

Palmer, C. J., A. L. Thorsten, L. J. Carpenter, F. C. Kupper, and G. B. McFiggans (2005), Iodine and halocarbon response of *Laminaria Digitata* to oxidative stress and links to atmospheric new particle production, *Environ. Chem.*, *2*, 282–290, doi:10.1071/EN05078.

Pedersén, M., J. Collén, K. Abrahamsson, and A. Ekdahl (1996), Production of halocarbons from seaweeds: An oxidative stress reaction, *Sci. Mar.*, *60*, 257.

Pszenny, A. A. P., W. C. Keene, D. J. Jacob, S. Fan, J. R. Maben, M. P. Zetwo, M. Springer-Young, and J. N. Galloway (1993), Evidence of inorganic chlorine gases other than hydrogen chloride in marine surface air, *Geophys. Res. Lett.*, *20*, 699–702, doi:10.1029/93GL00047.

Pszenny, A. A. P., J. Moldanova, W. C. Keene, R. Sander, J. R. Maben, M. Martinez, P. J. Crutzen, D. Perner, and R. G. Prinn (2004), Halogen cycling and aerosol pH in the Hawaiian marine boundary layer, *Atmos. Chem. Phys.*, *4*, 147–168.

Raofie, F., and P. A. Ariya (2003), Kinetics and products study of the reaction of BrO radicals with gaseous mercury, *J. Phys. IV*, *107*, 1119–1121, doi:10.1051/jp4:20030497.

Saiz-Lopez, A., and J. M. C. Plane (2004), Novel iodine chemistry in the marine boundary layer, *Geophys. Res. Lett.*, *31*, L04112, doi:10.1029/2003GL019215.

Saiz-Lopez, A., J. M. C. Plane, and J. A. Shillito (2004), Bromine oxide in the mid-latitude marine boundary layer, *Geophys. Res. Lett.*, *31*, L03111, doi:10.1029/2003GL018956.

Saiz-Lopez, A., J. M. C. Plane, G. McFiggans, P. I. Williams, S. M. Ball, M. Bitter, R. L. Jones, C. Hongwei, and T. Hoffmann (2006), Modelling molecular iodine emissions in a coastal marine environment: The link to new particle formation, *Atmos. Chem. Phys.*, *6*, 883–895.

Sander, R., and P. J. Crutzen (1996), Model study indicating halogen activation and ozone destruction in polluted air masses transported to the sea, *J. Geophys. Res.*, *101*, 9121–9138, doi:10.1029/95JD03793.

Sander, R., Y. Rudich, R. von Glasow, and P. J. Crutzen (1999), The role of $BrNO_3$ in marine tropospheric chemistry: A model study, *Geophys. Res. Lett.*, *26*, 2857–2860, doi:10.1029/1999GL900478.

Sander, R., et al. (2003), Inorganic bromine in the marine boundary layer: A critical review, *Atmos. Chem. Phys.*, *3*, 1301–1336.

Schall, C., and K. G. Heumann (1993), GC determination of volatile organoiodine and organobromine compounds in Arctic seawater and air samples, *Fresenius J. Anal. Chem.*, *346*, 717–722, doi:10.1007/BF00321279.

Schroeder, W. H., and J. Munthe (1998), Atmospheric mercury-An overview, *Atmos. Environ.*, *32*, 809–822, doi:10.1016/S1352-2310(97)00293-8.

Schweitzer, F., P. Mirabel, and C. George (1998), Multiphase chemistry of N_2O_5, $ClNO_2$, and $BrNO_2$, *J. Phys. Chem. A*, *102*, 3942–3952, doi:10.1021/jp980748s.

Shon, Z.-H., K.-H. Kim, M.-Y. Kim, and M. Lee (2005), Modeling study of reactive gaseous mercury in the urban air, *Atmos. Environ.*, *39*, 749–761, doi:10.1016/j.atmosenv.2004.09.071.

Shon, Z.-H., K.-H. Kim, S.-K. Song, M.-Y. Kim, and J. S. Lee (2008), Environmental fate of gaseous elemental mercury at an urban monitoring site based on long-term measurements in Korea (1997–2005), *Atmos. Environ.*, *42*, 142–155, doi:10.1016/j.atmosenv.2007.09.008.

Siegel, M. W., and W. L. Fite (1976), Terminal ions in weak atmospheric pressure plasmas. Applications of atmospheric pressure ionization to trace impurity analysis in gases, *J. Phys. Chem.*, *80*(26), 2871–2881, doi:10.1021/j100567a013.

Singh, H. B., et al. (1996), Low ozone in the marine boundary layer of the tropical Pacific Ocean: Photochemical loss, chlorine atoms, and entrainment, *J. Geophys. Res.*, *101*, 1907–1917, doi:10.1029/95JD01028.

Spicer, C. W., E. G. Chapman, B. J. Finlayson-Pitts, R. A. Pastridge, J. M. Hubbe, J. D. Fast, and C. M. Berkowitz (1998), Unexpectedly high concentrations of molecular chlorine in coastal air, *Nature*, *394*, 353–356, doi:10.1038/28584.

Spicer, C. W., R. A. Plastridge, K. L. Foster, B. J. Finlayson-Pitts, J. W. Bottenheim, A. M. Grannas, and P. B. Shepson (2002), Molecular halogens before and during ozone depletion events in the Arctic at polar sunrise: Concentrations and sources, *Atmos. Environ.*, *36*, 2721–2731, doi:10.1016/S1352-2310(02)00125-5.

Stutz, J., R. Ackermann, J. D. Fast, and L. Barrie (2002), Atmospheric reactive chlorine and bromine at the Great Salt Lake, Utah, *Geophys. Res. Lett.*, *29*(10), 1380, doi:10.1029/2002GL014812.

Tanaka, P. L., et al. (2003), Direct evidence for chlorine-enhanced urban ozone formation in Houston, Texas, *Atmos. Environ.*, *37*, 1393–1400, doi:10.1016/S1352-2310(02)01007-5.

Tellinghuisen, J. (2003), Precise equilibrium constants from spectrophotometric data: BrCl in Br_2/Cl_2 gas mixtures, *J. Phys. Chem. A*, *107*, 753–757, doi:10.1021/jp027227w.

Truesdale, V. W., and C. Canosamas (1995), Kinetics of disproportionation of hypoidous acid in phosphate and borate buffer at pH <8.5 modeled using iodide feedback, *J. Chem. Soc. Faraday Trans.*, *91*, 2269–2273, doi:10.1039/ft9959102269.

Vogt, R., P. J. Crutzen, and R. Sander (1996), A mechanism for halogen release from seasalt aerosol in the remote marine boundary layer, *Nature*, *383*, 327–330, doi:10.1038/383327a0.

Vogt, R., R. Sander, R. von Glasow, and P. Crutzen (1999), Iodine chemistry and its role in halogen activation and ozone loss in the marine boundary layer: A model study, *J. Atmos. Chem.*, *32*, 375–395, doi:10.1023/A:1006179901037.

Volpe, C., M. Wahlen, A. A. P. Pszenny, and A. J. Spivack (1998), Chlorine isotopic composition of marine aerosols: Implications for the release of reactive chlorine and HCl cycling rates, *Geophys. Res. Lett.*, *25*, 3831–3834, doi:10.1029/1998GL900038.

von Glasow, R., R. Sander, A. Bott, and P. J. Crutzen (2002), Modeling halogen chemistry in the marine boundary layer: 1. Cloud free MBL, *J. Geophys. Res.*, *107*(D17), 4341, doi:10.1029/2001JD000942.

Wei, Y. J., C. G. Liu, and L. P. Mo (2005), Ultraviolet absorption spectra of iodine, iodide ion and triiodide ion, *Guang Pu Xue Yu Guang Pu Fen Xi*, *25*, 86–88.

Wingenter, O. W., D. R. Blake, N. J. Blake, B. C. Sive, F. S. Rowland, E. Atlas, and F. Flocke (1999), Tropospheric hydroxyl and atomic chlorine concentrations and mixing timescales determined from hydrocarbon and halocarbon measurements made over the Southern Ocean, *J. Geophys. Res.*, *104*, 21,819–21,828, doi:10.1029/1999JD900203.

Yvon, S. A., E. S. Saltzman, D. J. Cooper, T. S. Bates, and A. M. Thompson (1996), Atmospheric sulfur cycling in the tropical Pacific marine boundary layer (12°S, 135°W): A comparison of field data and model results—1. dimethylsulfide, *J. Geophys. Res.*, *101*, 6899–6909, doi:10.1029/95JD03356.

B. D. Finley and E. S. Saltzman, Department of Earth System Science University of California, Irvine, CA 92697, USA. (bfinley@uci.edu)